

Heuristic Optimization of Bone Cement Distribution for Prevention of Osteoporotic Hip Fractures

María E. Santana Artiles and Demetrios T. Venetsanos

Abstract—Osteoporosis is a disease characterised by reduction of Bone Mineral Density (BMD) and micro-architectural deterioration of bone tissue. From all the osteoporotic fractures, hip fractures are the ones with most serious consequences. A new treatment to prevent these fractures is femoroplasty, consisting of the injection of bone cement into an osteoporotic femur in order to improve its mechanical properties. Injecting large amounts of cement can lead to bone thermal necrosis or create regions of stress concentration. The present study introduces a new evolutionary method for the optimization of the injected bone cement distribution and the minimization of its volume. The new method was numerically applied in a typical case of an osteoporotic femoral augmentation and compared to a powerful deterministic optimization method.

Index Terms—femoroplasty, biomechanics, optimization, bone augmentation.

I. INTRODUCTION

OVER two million people suffer from osteoporosis in the United Kingdom, meaning that approximately 300,000 osteoporotic fractures occur each year [1]. Hip fractures are cracks or breaks in the upper quarter of the femur bone. Among all the osteoporotic fractures, these are the ones with the most serious consequences, leading to surgery, disability and increase of the level of social dependency. Furthermore, the risk of mortality increases 20% the following year after an osteoporotic hip fracture [2].

Currently, preventive treatments for osteoporosis include protective devices, special diets, bone strengthening exercises and drugs. These treatments have shown to reduce the risk of fractures [3], although they are limited by side effects and long delays in restoring bone properties. An alternative preventive intervention to reduce the risk of hip osteoporotic fractures is femoroplasty. It is a procedure in research stage that involves augmentation of the proximal femur by injecting agents such as polymethylmethacrylate (PMMA) bone cement. However, large amounts of cement can lead to thermal necrosis, due to the exothermic reaction generated in the curing process, and embolism if bone cement is leaked into the blood vessels.

Most of experimental tests regarding femoroplasty have been carried out using gross filling of the femoral neck and trochanter, about 40-50ml of cement [4]. They have shown a significant increase in the fracture load, but also an increase of bone surface temperature. Some other in-vitro

experiments have been performed limiting the cement volume and modifying the injection technique. This is the case of [5], who reduced the cement volume but damaged the bone cortex due to the injection procedure. Fliri et al. [6] injected on average of 10.8ml of bone cement using a V-shaped augmentation technique that increased the fracture energy, but did not affect the yield load. In a recent study, [7] designed and tested a patient specific treatment for femoroplasty, proving that 9ml of cement are enough to increase the fracture load of an osteoporotic femur by 30%. Based on the aforementioned literature references, it is evident that the optimization of the volume and the distribution of bone cement in a femoroplasty comprises a contemporary state of the art problem. Within this framework, the present work introduces a new heuristic algorithm for the optimization of the injected bone cement distribution and the minimization of its volume. To test the performance of the newly introduced method, a comparison against the results obtained using a deterministic optimization technique was also conducted.

II. METHODS

A. Model development

The development of the model was achieved following the steps which are described in the next paragraphs.

Step 1: Retrieve CT scans of a femur

CT images of a healthy femur were obtained from the OsiriX open access repository (<http://www.osirix-viewer.com/datasets/>), the policy of which allows the use of the available files for research and teaching purposes. For the needs of the present work, a set of CT images in DICOM format was downloaded from OsiriX.

Step 2: Extract geometry for femur

To extract the three dimensional geometry of the femur, the downloaded set of CT images from Step 1 was segmented using InVesalius 3.0. This is an open source software for reconstruction of 3D medical images developed by Centro de Tecnologia de Informaçao Renato Archer (CTI), in Brazil. As an output of this step, an STL file of a femoral bone was exported from InVesalius 3.0.

Step 3: Develop 3D CAD solid model for femur

The STL file from Step 2 was imported into the commercial CAD software SolidWorks. Appropriate CAD surface techniques were applied and a 3D solid model was developed. As an output of this step, an IGES file with the 3D CAD solid model was exported from SolidWorks.

Manuscript received March 18, 2016; revised April 10, 2016.

María E. Santana Artiles, Kingston University London, e-mail: k1436463@kingston.ac.uk

Demetrios T. Venetsanos, Kingston University London, e-mail: D.Venetsanos@kingston.ac.uk

Step 4: Create mesh for the femur 3D CAD solid model

The IGES file from Step 3 was imported into the commercial FEA software ANSYS (Mechanical APDL ver.16). For the discretization of the solid model, an unstructured mesh was generated using 10-node tetrahedral elements. A Linear Static (LS) analysis, of a typical load case describing a fall, was conducted. The mesh finally selected for the present paper was obtained through a mesh-convergence study, based on which the average element size was found to be 7mm for the proximal femur and 20mm for the rest of the bone, respectively, totaling 21608 nodes and 112525 elements. As an output of this step, an Ansys ASCII archive (.cdb) file with the Finite Element mesh of the examined femur was created.

Step 5: Assign healthy bone properties to the meshed femur model

For the needs of this step, the freeware Bonemat ver.3.1 [8] was used. Bonemat is a freeware that maps, on a Finite Element (FE) mesh, bone elastic properties derived from Computed Tomography images (<http://www.bonemat.org/>). For the present study, the files used were the Ansys ASCII archive file (.cdb) with the FE mesh from Step 4 and the DICOM files from Step 1. As an output of this step, an updated Ansys ASCII archive file was created, corresponding to a healthy femur, with bone material properties being assigned separately to each element of the FE mesh.

Step 6: Assign osteoporotic bone properties to the meshed femur model

Step 5 was repeated, this time implementing material properties of an osteoporotic bone. To this end, Eqs.(2,3,4) were used for the determinations of the Young's modulus. As an output of this step, another Ansys ASCII archive file was created, corresponding to an osteoporotic femur.

As mentioned before, for Steps 5 and 6, it was necessary to map inhomogeneous material properties from the CT images into the FE model using the Bonemat v3.1 software. The Bonemat code converts each Hounsfield Unit (HU) value into a Young's modulus (E) value through several relationships and then performs a numerical integration over each element's volume to calculate the average Young's modulus [9].

First, the radiological density (ρ_{QCT}) was obtained from the CT densitometric calibration. CT datasets are usually calibrated using a calibration phantom. However, there was no scanner calibration available for the used files and this relation was defined in agreement with information from the images and the literature. The images belonged to a non-osteoporotic man and the HU range of bone tissue varied from -100 to 1500 (evaluated in the software InVesalius). Besides, the average Young's modulus of a healthy femur can be considered 16GPa for cortical bone and 5GPa for trabecular bone [10]. With this, it was possible to determine a reasonable CT densitometric calibration equation for a healthy femur (Eq. 1):

$$\rho_{QCT(H)} = 0.109 + 0.001086 \cdot HU \quad (1)$$

Where $\rho_{QCT(H)}$ is the radiological density of the healthy bone and HU is the Hounsfield Unit value.

However, in this work it was desired to represent both

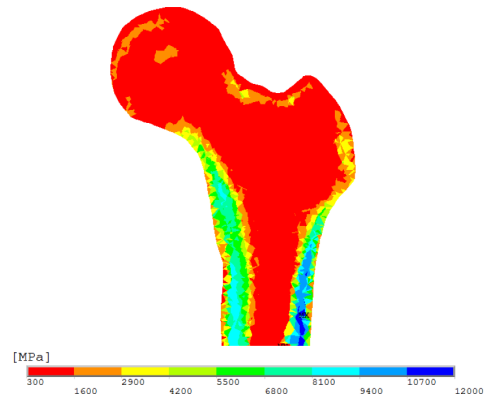


Fig. 1. Distribution of Young's modulus in the osteoporotic bone derived from CT scan data

healthy and osteoporotic femur in the finite element models. The available CT scan and thus, Eq. 1 belong to a healthy bone. In order to create the model of the osteoporotic bone, it was necessary to apply the definition of osteoporosis. According to the World Health Organization, an osteoporotic bone presents Bone Mineral Density (BMD) more than 2.5 Standard Deviations below the adult mean value. The femur neck BMD of a young, normal adult population was estimated to be 1.02g/cm² (SD=0.144) [11]. Therefore, an osteoporotic bone will present a BMD of 0.66g/cm² or below, meaning a reduction of 35%. For this reason, Eq. 1 was reduced by 35% (Eq. 2):

$$\rho_{QCT(O)} = 0.0712 + 0.0007058 \cdot HU \quad (2)$$

The relationship between radiological density (ρ_{QCT}) and ash density (ρ_{ash}) was defined according to Schileo et al. [9] (Eq. 3):

$$\rho_{ash} = 0.079 + 0.88 \cdot \rho_{QCT} \quad (3)$$

The density-elasticity relationship (Eq. 4) was taken from the work of Keller [12]:

$$E = 10.500 \cdot \rho_{ash}^{2.29} \quad (4)$$

In this relationship, E (Young's modulus) is expressed in GPa when ρ_{ash} (ash density) is expressed in g/cm³.

Finally, a Poisson's ratio of 0.3 was assumed for all the elements and a modulus step size of 100MPa was set to control the number of different materials to generate. The material distribution of the osteoporotic bone is shown in Fig. 1

The average values of the Young's modulus for the healthy bone were 17GPa and 2.5GPa for cortical and trabecular respectively. Similarly, 7.5GPa and 1GPa were the resulting values for the osteoporotic femur.

B. Yield load prediction

In order to predict the yield load in a finite element analysis, a yield criterion has to be adopted. There are different criteria that have been used in several studies, including von Mises, Drucker-Prager, maximum principal strain and maximum principal stress although there is still no general agreement on the most suitable criteria to use. Keyak et al. [13] showed that the distortion energy theories were the most robust ones. Later, [14] and [15] found that

the strain criterion is the most accurate method for yield load prediction and fracture location. Having considered this, the adopted criterion for this work was a strain-based yield criterion.

First, the femur was oriented according to the reference system, which is based on three skeletal landmarks: head centre and two epicondyles (Fig. 2). Boundary conditions replicating a lateral fall onto the greater trochanter were applied to the models. The femur was distally constrained and the lateral side of the greater trochanter was restricted to move only in one plane [16]. Load was uniformly distributed among the surface nodes of the medial part of the femoral head and the magnitude was initially set to an arbitrary value of 1000N. Furthermore, the force direction was tilted 10° in the transverse plane and 15° in the frontal plane, as can be seen in Fig. 2. This is the most used configuration to replicate lateral falls in the literature [17].

Principal strains can be positive (tensile) or negative (compressive). Hence, for each element of the region of interest (proximal femur), the maximum (ϵ_{max}) and minimum (ϵ_{min}) principal strains were computed. Then, the greater value of $|\epsilon_{max}|$ and $|\epsilon_{min}|$ was chosen and compared with the appropriate yield strain: 0.73% in tension and -1.04% in compression [10]. If the element strain exceeded the limit value, it was considered a failed element. The load was increased gradually and the analysis was performed until 1% of the elements of the region of interest failed, reaching the yield load of the bone. The finite element analyses were performed with ANSYS ver.16 (Ansys Inc, PA, USA) for both models: healthy and osteoporotic bone.

C. Optimization

The optimization problem in bone augmentation may be stated as finding the locations where bone cement must be injected, so that a predetermined level of reinforcement is achieved by using the minimum amount of bone cement. Since bone cement is not injected in the cortical tissue, the candidate locations for injection are related only to the trabecular tissue. In such a problem statement, the size of the design vector is very large as it includes all

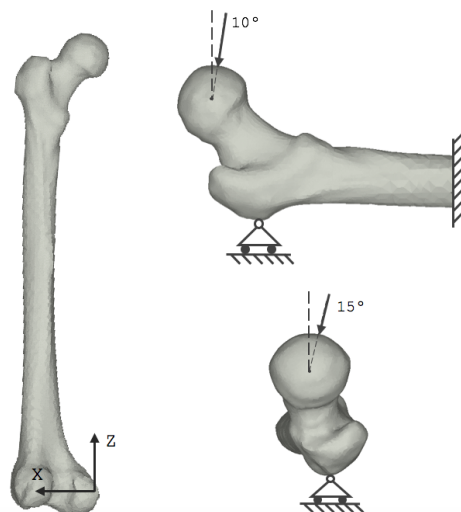


Fig. 2. Reference system (left) and representation of the loading conditions (right)

elements used for the discretization of the trabecular tissue. Theoretically, any deterministic or stochastic optimization scheme may be used but the size of the design vector increases significantly the computational cost. Alternatively, a heuristic optimization method may be developed.

The present paper introduces a heuristic unidirectional iterative evolutionary scheme. More particularly, at each iteration, the weakest elements of the trabecular tissue are detected and their material properties are changed into the material properties of PMMA bone cement (elastic modulus: 2300MPa; Poisson's ratio: 0.3 [18], [19]). The procedure continues until a predetermined level of reinforcement is achieved. In the present paper, this level is described as the bone obtaining the load capacity of its prior healthy condition. The pseudocode of the proposed procedure is presented below and it was developed as a code written in the ANSYS Parametric Design Language (APDL). For comparison, another optimization scheme was used, the pseudocode of which is also included in this Section. The corresponding code was developed in MatLab, implementing the intrinsic optimization function "fmincon", which utilizes the deterministic Sequential Quadratic Programming scheme.

1) New Heuristic Optimization Method: In this scheme, there are two parameters controlling, respectively, the load step and the percentage of elements to sustain a change in material properties. The values of these parameters were set equal to 10% and 1%, respectively.

Set up the model for a Linear Static (LS) analysis

Define Region of Interest (ROI)

Define applied load as a small fraction of the healthy yield load

While applied load < yield load of healthy bone Do

While Failed elements < 1% Do

Conduct a Linear Static FE analysis

Find elements violating strain criterion

Failed elements=Violating elements/Total elements in the ROI

Increase load by 10%

End (failed elements)

Assign bone cement material properties to failed elements

End (load)

Obtain optimum bone cement volume

2) MatLab Optimization: The second optimization procedure used ANSYS as the FEA solver and MatLab as the optimization solver. In this analysis, the applied load was constant and similar to the healthy femur yield load:

Initialize the number of cemented elements in MatLab

Conduct a Linear Static (LS) FE analysis in ANSYS

Evaluate if minimum was found (fmincon function)

While minimum NOT found Do

New fmincon estimation: number of cemented elements

Call ANSYS as external solver and conduct a (LS) FE analysis

Import failed elements to MatLab

If failed elements < 1%:

Fmincon evaluates if minimum was found

Else

Constraint violated: minimum not found

End

Obtain optimum bone cement volume

III. RESULTS

The femur yield load of both a healthy and an osteoporotic bone was calculated in the first analysis. A force of 2662N was needed to load 1% of the elements of the proximal osteoporotic femur beyond their strain limits. Similarly, the load had to be increased to 5500N in order to achieve the same in the healthy bone.

In both femora, the largest strains due to a fall into the greater trochanter occurred in the superior side of the neck region, where compressive strains were larger than the tensile ones. Compression dominated on the lateral side of the femur, while tension was mainly found in the medial side; specifically in the lower part of the neck. Trabecular and cortical tissue contributed to bone strength similarly in both analyses; generating similar strain distributions in the proximal femur. According to the ANSYS optimization results, 11.7ml of cement were needed in order to increase the yield load of the osteoporotic bone to the approximate same one of the healthy bone. 19 iterations were performed to reach the final yield load, although cement was only added when 1% of elements were beyond the strain limits.

Fig. 3 shows the two lines that define the bounds of the PMMA volume that can be injected in the osteoporotic femur. The upper line represents the most conservative approach, according to which a certain yield load has been achieved and no element violates the imposed constraints on the strains. The lower line represents an approach, according to which the aforementioned yield load has been achieved but a very small fraction of elements is allowed to violate the imposed constraints. This small fraction is user-defined (in the present paper, it was set equal to 1%) and its presence can be justified due to numerical reasons.

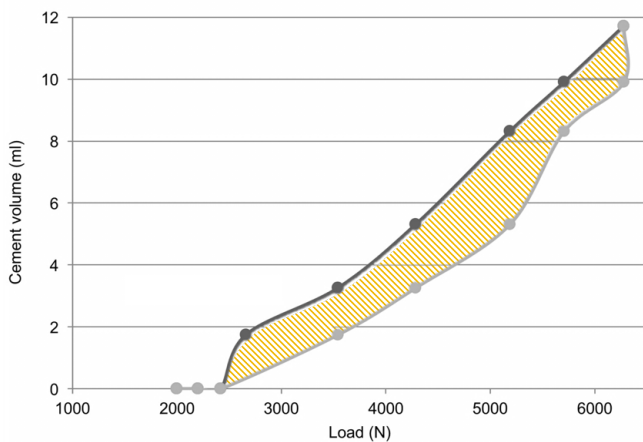


Fig. 3. Load-Cement volume graph

The evolution of cement distribution in ANSYS is illustrated in Fig. 4. The optimization algorithm started adding elements in the greater trochanter, which is the area with largest principal strains. After this, the superior part of the femoral neck is reinforced, starting the formation of a ring around the neck. The inferior side of the neck is cemented independently until the last iteration, where the two augmented volumes join together. From this it can be inferred that for the applied boundary conditions cement should be placed mainly in the greater trochanter area and around the femoral neck.

TABLE I
OPTIMIZATION RESULTS

Case	Initial Volume	Final Volume	CPU time
Heuristic Method	0ml	11.7ml	<5min
MatLab A	3.21ml	27.54ml	>85min
MatLab B	9.63ml	26.06ml	>55min
MatLab C	12.84ml	25.11ml	>60min
MatLab D	22.48ml	27.28ml	>50min

Four optimizations were performed in MatLab varying the design vector in order to check that results are independent of the initial guess. Hence, taking into consideration the four optimizations, the average optimum cement volume was 26.62ml (Table I). In general, the MatLab optimization converged to a realistic solution in all the cases, with a maximum difference of 2.7ml of cement between results.

In all the four cases, the solver stopped because the optimality criteria were satisfied, meaning that a local minimum was found. Case A presented the slowest convergence, needing eight iterations and 115 function evaluations, while the rest of cases needed seven iterations and 90 function evaluations. Regarding the final PMMA volume, Case C was the one requiring the smallest amount of cement (25.11ml), while Case A was the one requiring the largest amount (27.54ml). Despite this difference, all the optimizations sculpted the cement in the bone in the same manner and there are not any major variations between all the distributions.

IV. DISCUSSION

The first stage in this work was to develop a 3D reconstruction of the femur based on a CT scan of the human body. It is widely accepted that bone presents anisotropic behaviour but in order to simulate this, inhomogeneous isotropic material properties are commonly mapped from the CT scan to the FE mesh [20]. Thus, patient-specific FE models of any bone can be created and used to predict its behaviour. However, despite this is a commonly used methodology, the most adequate relationship between bone density and modulus of elasticity remains unclear. The most referenced equations for this purpose are the ones of [12] and [21] shown in Eq. 5 and 6 respectively.

$$E = 10.500 \cdot \rho_{ash}^{2.29} \quad (5)$$

$$E = 3.790 \cdot \rho_{app}^3 \quad (6)$$

In a more recent study, [22] proved that the density-elasticity relationship highly depends on the anatomic location, presenting new equations for the femoral greater trochanter and femoral neck (Eq. 7).

$$E = 6.950 \cdot \rho_{app}^{1.49} \quad (7)$$

Schileo et al. [14] compared Eq. 5, 6 and 7. This investigation suggested that the relationship presented by [22] was the most accurate one to predict strains in the proximal femur, while equations 5 and 6 overestimated the predicted strains. In this study, a model of the whole femur (not just the proximal part) was created so Eq. 5 was applied. However, it could be of interest to combine

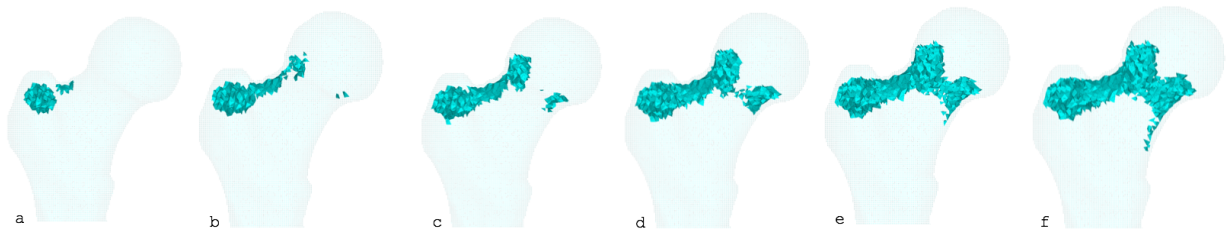


Fig. 4. Evolution of the cement in ANSYS (from a to f)

equations 5 and 7 to develop a more accurate model.

Once the model was created, it was necessary to adopt a criterion to predict the yield load using FEA. Some studies use stress-based fracture criterion like von Mises [13]. Others agree that the Drucker-Prager yield criterion is more suitable than von Mises in FE models that simulate brittle materials such as bone [23]. Finally, some others have shown that bone fracture is a strain-controlled mechanism [24], [25]. Schileo et al. [9] performed a numerical-experimental study comparing a strain criterion with two different stress criteria to determine the femur failure load. Their results, in agreement with [15] suggest that the failure load would be underestimated when using von Mises or principal stress criteria. For this reason, in this work the femur yield load was predicted evaluating principal strains. It has also been reported that bone fails at lower strains in tension than in compression [10], hence the assumption of $\varepsilon_{max} = 0.73\%$ and $\varepsilon_{min} = -1.04\%$.

Regarding loading conditions, in literature they range from stance, single limb stance or fall to the side [17], [26]. Nevertheless, most osteoporotic hip fractures occur as a result of a fall to the side, so this study was focused only on this specific loading condition. In addition, most of in-vitro experiments replicate a lateral fall in order to predict the fracture load of osteoporotic femora.

Several publications show the use of finite element analysis in order to estimate bone strength. Falcinelli et al. [26] studied the yield load of osteoporotic femora under different fall loading conditions. Comparing their results with the ones of this study, there is a difference of 7% between them. In a different study, [27], used micro-FE models to compare the yield load of a healthy and an osteoporotic femur during a fall to the side. The osteoporotic femur yield load obtained by [27] is significantly larger than the one obtained in this work. However, the healthy femur yield load is very similar to the one presented here.

Furthermore, it was found that the predicted yield loads of this project were in a reasonable range and corresponded well with values based on femoral BMD values: range of 5-10kN for healthy and 1-5kN for osteoporotic proximal femur [28]. Besides the yield load, the failure pattern of the femur was also addressed in this work. The strains that induced the fracture of the bone occurred in the superior side of the neck region and were mainly compressive, in agreement with [29].

The reported predictions were made considering that the femur yield load was achieved if 1% of the elements of the region of interest were above the strain limit values. This value of 1% was adopted by [17] as well, although other authors consider that a value of 2% is more realistic to

assess bone strength [27]. Different approaches have been presented in literature as in the case of [26] who averaged the principal strains on a circle of 3mm radius and [15], who focused their analysis on the 10 elements most susceptible to failure.

The optimization of cement volume and distribution was performed using two different methods. First, a heuristic optimization program that was written in APDL and second, a deterministic method using MatLab. In ANSYS, the applied load increased progressively as the femur was reinforced. However, in MatLab the desired yield load was an imposed condition and the femur was augmented using only the strain state of this configuration. This is one of the reasons for the significant difference between the results achieved with each technique. ANSYS optimization required less than half of the cement needed in the MatLab optimization. Furthermore, ANSYS optimization needed less cement in the greater trochanter area and the inferior aspect of the femoral neck. Therefore, this suggests that the new evolutionary scheme developed in APDL suits best this specific problem. Besides this, the ANSYS optimization required considerably less computational time than the MatLab one.

Despite the numerical differences, all the optimizations placed the cement in similar locations: femoral neck and greater trochanter. These results are in agreement with in-vitro experiments on femur [15], which have found that the initial failure happens at the superior aspect of the femoral neck under lateral fall loading conditions.

Therefore, this study suggests that less than 12ml of cement could theoretically increase the femur yield load by more than 100%. In previous experiments, around 40-50ml of cement were used, obtaining only 30-40% increase in the fracture load [4], [30]. This difference confirms the importance of the augmentation material localization.

In contrast to these studies, some recent researches have evaluated the femoroplasty procedure performing in vitro cadaveric studies and using a considerably lower amount of cement. Beckmann et al. [5] evaluated different cementing techniques to determine the most appropriate one. They concluded that cement augmentation in the centrodorsal aspect of the head and neck was more efficient than the other methods and needed an average of 12ml of bone cement. This cement placement involves augmenting all the femoral neck region but not the greater trochanter, so it is different to the distribution achieved in this study.

The cement pattern *sculpted* in the bone by the APDL code involved augmenting the greater trochanter and creating a ring of cement around the femoral neck. This distribution is similar to the one reached by [17]. However, injecting

the exact simulated cement pattern in a real femur might be unfeasible due to the limitations when placing cement inside of the bone. Hence, in a recent study conducted by [7], the cement injection procedure was simulated to create a realistic injection pattern and they tested eight femora in an experimental verification study.

V. CONCLUSION

A new heuristic evolutionary method was introduced for the optimization of bone augmentation. As an application, the reinforcement of a proximal femur with bone cement was examined and the performance of the method was compared to that of a powerful deterministic optimization procedure. The proposed method required much less time to achieve an increase of 100% in the yield load by converging to a bone cement volume (12ml), which is significantly lower than the best value (ca 25ml) obtained with the deterministic optimization procedure. Consequently, the simplicity and performance of the proposed method suggest its suitability as a tool to develop an efficient treatment for prevention of osteoporotic hip fractures through an optimized bone augmentation.

REFERENCES

- [1] S. Ishtiaq, I. Fogelman, and G. Hampson, "Treatment of postmenopausal osteoporosis: Beyond bisphosphonates," *Journal of endocrinological investigation*, vol. 38, no. 1, pp. 13–29, 2015.
- [2] C. L. Leibson, A. N. A. Tosteson, S. E. Gabriel, J. E. Ransom, and L. J. Melton, "Mortality, disability, and nursing home use for persons with and without hip fracture: A population-based study," *Journal of the American Geriatrics Society*, vol. 50, no. 10, pp. 1644–1650, 2002.
- [3] J. A. Kanis, "Osteoporosis iii: Diagnosis of osteoporosis and assessment of fracture risk," *Lancet*, vol. 359, no. 9321, pp. 1929–1936, 2002.
- [4] J. Beckmann, S. J. Ferguson, M. Gebauer, C. Luering, B. Gasser, and P. Heini, "Femoroplasty - augmentation of the proximal femur with a composite bone cement - feasibility, biomechanical properties and osteosynthesis potential," *Medical Engineering and Physics*, vol. 29, no. 7, pp. 755–764, 2007.
- [5] J. Beckmann, R. Springorum, E. Vettorazzi, S. Bachmeier, C. L. üring, M. Tingart, K. P. üschel, O. Stark, J. Grifka, T. Gehrke, M. Amling, and M. Gebauer, "Fracture prevention by femoroplasty-cement augmentation of the proximal femur," *Journal of Orthopaedic Research*, vol. 29, no. 11, pp. 1753–1758, 2011.
- [6] L. Fliri, A. Sermon, D. Whnert, W. Schmoelz, M. Blauth, and M. Windolf, "Limited v-shaped cement augmentation of the proximal femur to prevent secondary hip fractures," *Journal of Biomaterials Applications*, vol. 28, no. 1, pp. 136–143, 2013.
- [7] E. Basafa, R. J. Murphy, Y. Otake, M. D. Kutzer, S. M. Belkoff, S. C. Mears, and M. Armand, "Subject-specific planning of femoroplasty: An experimental verification study," *Journal of Biomechanics*, vol. 48, no. 1, pp. 59–64, 2015.
- [8] F. Taddei, E. Schileo, B. Helgason, L. Cristofolini, and M. Viceconti, "The material mapping strategy influences the accuracy of ct-based finite element models of bones: An evaluation against experimental measurements," *Medical Engineering and Physics*, vol. 29, no. 9, pp. 973–979, 2007.
- [9] E. Schileo, E. Dall'Ara, F. Taddei, A. Malandrino, T. Schotkamp, M. Baleani, and M. Viceconti, "An accurate estimation of bone density improves the accuracy of subject-specific finite element models," *Journal of Biomechanics*, vol. 41, no. 11, pp. 2483–2491, 2008.
- [10] H. H. Bayraktar, E. F. Morgan, G. L. Niebur, G. E. Morris, E. K. Wong, and T. M. Keaveny, "Comparison of the elastic and yield properties of human femoral trabecular and cortical bone tissue," *Journal of Biomechanics*, vol. 37, no. 1, pp. 27–35, 2004.
- [11] A. C. Looker, L. G. Borrud, J. P. Hughes, B. Fan, J. A. Shepherd, and L. J. Melton, "Lumbar spine and proximal femur bone mineral density, bone mineral content, and bone area: United states, 2005–2008," *Vital and health statistics.Series 11, Data from the national health survey*, no. 251, pp. 1–132, 2012.
- [12] T. S. Keller, "Predicting the compressive mechanical behavior of bone," *Journal of Biomechanics*, vol. 27, no. 9, pp. 1159–1168, 1994.
- [13] J. H. Keyak, S. A. Rossi, K. A. Jones, C. M. Les, and H. B. Skinner, "Prediction of fracture location in the proximal femur using finite element models," *Medical Engineering and Physics*, vol. 23, no. 9, pp. 657–664, 2001.
- [14] E. Schileo, F. Taddei, A. Malandrino, L. Cristofolini, and M. Viceconti, "Subject-specific finite element models can accurately predict strain levels in long bones," *Journal of Biomechanics*, vol. 40, no. 13, pp. 2982–2989, 2007.
- [15] Z. Yosibash, D. Tal, and N. Trabelsi, "Predicting the yield of the proximal femur using high-order finite-element analysis with inhomogeneous orthotropic material properties," *Philosophical Transactions of the Royal Society A: Mathematical, Physical and Engineering Sciences*, vol. 368, no. 1920, pp. 2707–2723, 2010.
- [16] E. Schileo, L. Balistreri, L. Grassi, L. Cristofolini, and F. Taddei, "To what extent can linear finite element models of human femora predict failure under stance and fall loading configurations?" *Journal of Biomechanics*, vol. 47, no. 14, pp. 3531–3538, 2014.
- [17] E. Basafa and M. Armand, "Subject-specific planning of femoroplasty: A combined evolutionary optimization and particle diffusion model approach," *Journal of Biomechanics*, vol. 47, no. 10, pp. 2237–2243, 2014.
- [18] M. Kinzl, A. Boger, P. K. Zysset, and D. H. Pahr, "The mechanical behavior of pmmma/bone specimens extracted from augmented vertebrae: A numerical study of interface properties, pmmma shrinkage and trabecular bone damage," *Journal of Biomechanics*, vol. 45, no. 8, pp. 1478–1484, 5/11 2012.
- [19] Y. Lu, G. Maquer, O. Museyko, K. Püschel, K. Engelke, P. Zysset, M. Morlock, and G. Huber, "Finite element analyses of human vertebral bodies embedded in polymethylmethacrylate or loaded via the hyperelastic intervertebral disc models provide equivalent predictions of experimental strength," *Journal of Biomechanics*, vol. 47, no. 10, pp. 2512–2516, 2014.
- [20] G. Chen, B. Schmutz, D. Epari, K. Rathnayaka, S. Ibrahim, M. A. Schuetz, and M. J. Pearcy, "A new approach for assigning bone material properties from ct images into finite element models," *Journal of Biomechanics*, vol. 43, no. 5, pp. 1011–1015, 3/22 2010.
- [21] D. R. Carte and W. C. Hayes, "The compressive behavior of bone as a two-phase porous structure," *Journal of Bone and Joint Surgery - Series A*, vol. 59, no. 7, pp. 954–962, 1977.
- [22] E. F. Morgan, H. H. Bayraktar, and T. M. Keaveny, "Trabecular bone modulus-density relationships depend on anatomic site," *Journal of Biomechanics*, vol. 36, no. 7, pp. 897–904, 2003.
- [23] M. Bessho, I. Ohnishi, J. Matsuyama, T. Matsumoto, K. Imai, and K. Nakamura, "Prediction of strength and strain of the proximal femur by a ct-based finite element method," *Journal of Biomechanics*, vol. 40, no. 8, pp. 1745–1753, 2007.
- [24] S. P. Väänänen, S. A. Yavari, H. Weinans, A. A. Zadpoor, J. S. Jurvelin, and H. Isaksson, "Repeatability of digital image correlation for measurement of surface strains in composite long bones," *Journal of Biomechanics*, vol. 46, no. 11, pp. 1928–1932, 7/26 2013.
- [25] R. K. Nalla, J. S. Stölken, J. H. Kinney, and R. O. Ritchie, "Fracture in human cortical bone: Local fracture criteria and toughening mechanisms," *Journal of Biomechanics*, vol. 38, no. 7, pp. 1517–1525, 2005.
- [26] C. Falcinelli, E. Schileo, L. Balistreri, F. Baruffaldi, B. Bordini, M. Viceconti, U. Albisinni, F. Ceccarelli, L. Milandri, A. Toni, and F. Taddei, "Multiple loading conditions analysis can improve the association between finite element bone strength estimates and proximal femur fractures: A preliminary study in elderly women," *Bone*, vol. 67, pp. 71–80, 2014.
- [27] E. Verhulp, B. van Rietbergen, and R. Huiskes, "Load distribution in the healthy and osteoporotic human proximal femur during a fall to the side," *Bone*, vol. 42, no. 1, pp. 30–35, 2008.
- [28] X. G. Cheng, G. Lowet, S. Boonen, P. H. F. Nicholson, P. Brys, J. Nijs, and J. Dequeker, "Assessment of the strength of proximal femur in vitro: Relationship to femoral bone mineral density and femoral geometry," *Bone*, vol. 20, no. 3, pp. 213–218, 1997.
- [29] S. Majumder, A. Roychowdhury, and S. Pal, "Simulation of hip fracture in sideways fall using a 3d finite element model of pelvis-femur-soft tissue complex with simplified representation of whole body," *Medical Engineering and Physics*, vol. 29, no. 10, pp. 1167–1178, 2007.
- [30] E. G. Sutter, S. C. Mears, and S. M. Belkoff, "A biomechanical evaluation of femoroplasty under simulated fall conditions," *Journal of orthopaedic trauma*, vol. 24, no. 2, pp. 95–99, 2010.